

Multicast Capacity of Optical Packet Ring for Hotspot Traffic

Matthias an der Heiden, Michel Sortais, Michael Scheutzow, Martin Reisslein, *Senior Member, IEEE*,
Patrick Seeling, Martin Herzog, and Martin Maier, *Member, IEEE*

Abstract—Hotspot traffic is common in metro ring networks connecting access networks with backbone networks, and these metro rings are also expected to support a mix of unicast, multicast, and broadcast traffic. Shortest path (SP) routing, as employed in the IEEE 802.17 Resilient Packet Ring (RPR), is widely considered for metro rings as it maximizes spatial reuse and, thus, the achievable packet throughput (capacity) for uniform traffic. In this paper, we analyze the capacity of bidirectional optical ring networks, such as RPR, employing SP routing for multicast (nonuniform) hotspot traffic (whereby unicast and broadcast are considered as special cases of multicast). We find that, when the traffic originating at the hotspot exceeds a critical threshold, then SP routing leads to substantial reductions in capacity to a value close to one simultaneous packet transmission. To overcome this limitation of SP routing, we propose a simple combined SP/one-copy routing strategy that provides a capacity of at least two simultaneous packet transmissions.

Index Terms—Hotspot traffic, multicast, packet throughput, shortest path (SP) routing, spatial reuse.

I. INTRODUCTION

OPTICAL ring networks, such as the IEEE 802.17 Resilient Packet Ring (RPR) [1], aim to provide efficient yet simple packet-switched transport in metropolitan area networks [2]–[4]. One key mechanism for achieving high efficiency in optical ring networks is spatial reuse, whereby the destination node takes a packet off the ring, enabling the destination node or a node downstream to reuse the wavelength channel. Spatial reuse is maximized through shortest path (SP) routing, whereby the source node sends a packet in the ring direction that reaches the destination with the smallest hop distance, i.e., traversing the smallest number of intermediate network nodes.

Multicast traffic is expected to account for a significant portion of the metro area traffic due to growing applications, such as teleconferences [5], virtual private network interconnections, interactive distance learning, distributed games, and content distribution. These applications are expected to demand

substantial bandwidths due to the trend of delivering video and multimedia content in high-definition television (HDTV) format and the emergence of video formats with resolutions that are higher than HDTV for digital cinema and teleimmersion applications. While there is, at present, scant quantitative information about multicast traffic volume, there is ample anecdotal evidence of the emerging significance of this traffic type [6], [7]. As a result, multicasting has been identified as an important service in optical networks [8], [9] and has begun to attract significant attention in optical networking research, as outlined in Section I-A.

The RPR standard defines unidirectional flooding and bidirectional flooding for multicast traffic [1]. With unidirectional flooding, the source node sends the multicast packet in one ring direction all the way around the ring, whereas with bidirectional flooding, the packet is sent in both ring directions to a cleave point. With either strategy, a multicast packet traverses the entire ring, thus preventing spatial reuse for multicast traffic. A refined multicast transmission strategy is proposed and examined for uniform traffic in [10], whereby the source node sends the multicast packet in both directions to the multicast destination nodes bordering on the largest gap (LG) among the destination nodes. For uniform traffic, this refined strategy maximizes spatial reuse by avoiding traversal of the LG and thus maximizes the multicast capacity of the RPR network.

Metropolitan area networks consist typically of edge rings that interconnect several access networks (e.g., Ethernet passive optical networks) and connect to a metro core ring. The metro core ring interconnects several metro edge rings and connects to the wide area network. The node connecting a metro edge ring to the metro core ring is typically a traffic hotspot as it collects/distributes traffic destined to/originating from other metro edge rings or the wide area network. Similarly, the node connecting the metro core ring to the wide area network is typically a traffic hotspot. Examining the capacity of general optical packet-switched ring networks, including RPR, for hotspot traffic is therefore very important.

In this paper, we examine the capacity (maximum achievable long run average packet throughput) of bidirectional single-wavelength optical rings with a single hotspot for a general fan-out traffic model comprising unicast, multicast, and broadcast traffic. We consider an arbitrary traffic mix composed of uniform traffic, hotspot destination traffic (from regular nodes to the hotspot), and hotspot source traffic (from the hotspot to regular nodes). We first characterize and examine the capacity that is achieved with SP routing. We discover that SP routing does *not* maximize the capacity when the hotspot

Manuscript received July 5, 2006; revised June 3, 2007. This work was supported by the DFG Research Center MATHEON “Mathematics for Key Technologies,” Berlin, Germany.

M. an der Heiden, M. Sortais, and M. Scheutzow are with the Department of Mathematics, Technical University of Berlin, 10623 Berlin, Germany (e-mail: heiden@math.tu-berlin.de; sortais@math.tu-berlin.de; ms@math.tu-berlin.de).

M. Reisslein and P. Seeling are with the Department of Electrical Engineering, Arizona State University, Tempe, AZ 85287-5706 USA (e-mail: reisslein@asu.edu; patrick.seeling@asu.edu).

M. Herzog and M. Maier are with the Institut National de la Recherche Scientifique, Montréal, QC, H5A 1K6, Canada (e-mail: herzog@emt.inrs.ca; maier@ieee.org).

Digital Object Identifier 10.1109/JLT.2007.902092

source multicast traffic exceeds a critical threshold. This result is in contrast to uniform traffic, for which SP routing always provides the maximum capacity. To overcome the discovered limitation of SP routing, we propose and study a novel routing policy: When the hotspot source traffic is below the critical threshold, then SP routing is employed at all nodes; when the hotspot source traffic is above the threshold, then the hotspot routes its traffic according to a “one-copy (OC)” transmission strategy (detailed shortly), whereas all other nodes route their traffic according to the SP strategy. With this combined SP/OC routing strategy, the capacity is at least two (simultaneous packet transmissions in the network in the long run average) for any arbitrary traffic mix, whereas when only SP routing is employed, the capacity drops to one when there is a significant portion of hotspot source traffic. The proposed routing strategies are particularly relevant, as it appears that several emerging multicast applications, such as content distribution and Internet Protocol television (IPTV), will involve distribution of data from a hotspot.

This paper is organized as follows. Section I-A reviews related work. In Section II, we present our network and traffic models, and introduce our basic notation. In Section III, we analyze the maximum ring segment utilization probabilities and the resulting multicast capacity for SP routing. In Section IV, we introduce and examine the refined routing strategy that combines SP routing with the OC routing strategy. We summarize our conclusions in Section V.

A. Related Work

The analysis of the performance of optical packet rings, such as RPR, has received significant attention recently. Several studies have examined the fair bandwidth allocation in RPR and proposed refinements to enhance the fairness of RPR (see, e.g., [11]–[22]). The access delay, congestion control, and quality of service of RPR were examined in [23]–[26], while the protection performance was studied in [27]–[29].

Studies of nonuniform traffic in optical networks have generally focused on issues arising in circuit-switched optical networks (see, e.g., [30]–[36]). A comparison of circuit switching to optical burst switching network technologies, including a brief comparison for nonuniform traffic, was conducted in [37]. Capacity analyses of packet-switched optical ring networks have so far primarily focused on uniform packet traffic [10], [38]–[40]. In contrast, we consider nonuniform traffic with a hotspot node as it commonly arises in metro edge rings [41]. The throughput characteristics of a mesh network interconnecting routers on an optical ring through fiber shortcuts for nonuniform unicast traffic were examined in [42]. The study [43] considered the throughput characteristics of a ring network with uniform unicast traffic, where the nodes may adjust their send probabilities in a nonuniform manner. In contrast to these works, we consider a nonuniform traffic model with an arbitrary fan-out, which accommodates a wide range of unicast, multicast, and broadcast traffic mixes.

Multicasting in wavelength-division multiplexing (WDM) networks, including ring networks, has begun to attract significant attention [44], [45]. The photonic level issues that are

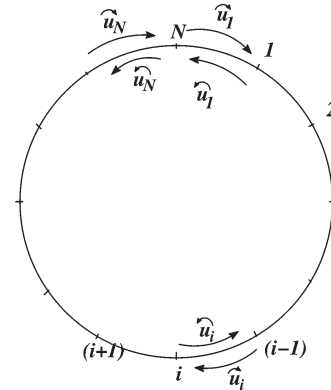


Fig. 1. Optical ring network model: N nodes are interconnected by one clockwise wavelength channel and one counterclockwise wavelength channel, each consisting of N segments.

involved in multicasting over ring WDM networks are explored in [46], while a node architecture for multicasting in WDM ring networks is studied in [47]. The general network architecture and MAC protocol issues arising from multicasting in packet-switched WDM ring networks are addressed in [48] and [49]. The capacity and delay performance of WDM rings for uniform multicast traffic are examined in [50] and [51]. We also note that a wide range of aspects of multicast in circuit-switched WDM ring and mesh networks has received considerable interest, such as light path design (see, e.g., [52] and [53]), traffic grooming (see, e.g., [54]), routing and wavelength assignment (see, e.g., [55] and [56]), and connection carrying capacity [57]. These studies do not address the stability limit (capacity) of a packet-switched optical ring network with a hotspot for multicast traffic, which is the main focus of this paper.

II. SYSTEM MODEL AND NOTATIONS

In our model of the optical packet ring network, we let N denote the number of nodes, which we index sequentially by $i, i = 1, \dots, N$, in the clockwise direction, as illustrated in Fig. 1. For $1 \leq i \leq N$, we let \hat{u}_i denote the clockwise-oriented ring segment connecting node $i - 1$ to node i . Analogously, we let \hat{u}_i denote the counterclockwise-oriented ring segment connecting node i to node $i - 1$.

Denote by S the node that is the sender. We introduce the random set of destinations (fan-out set) $\mathcal{F} \subset (\{1, 2, \dots, N\} \setminus \{S\})$. Moreover, we define the set of active nodes $\mathcal{A} := \mathcal{F} \cup \{S\}$.

We consider a traffic model combining a portion α of uniform traffic, a portion β of hotspot destination traffic, and a portion γ of hotspot source traffic, with $\alpha, \beta, \gamma \geq 0$, and $\alpha + \beta + \gamma = 1$.

- **Uniform traffic:** A given generated packet is a uniform traffic packet with probability α . For such a packet, the sending node is chosen uniformly at random among all network nodes $\{1, 2, \dots, N\}$. Once sender S is chosen, the number of receivers (also called fan-out) $l \in \{1, 2, \dots, N - 1\}$ is chosen at random according to a discrete probability distribution $(\mu_l)_{l=1}^{N-1}$. Once the fan-out l is chosen, the random set of destinations (fan-out

set) $\mathcal{F} \subset (\{1, 2, \dots, N\} \setminus \{S\})$ is chosen uniformly at random among all subsets of $\{1, 2, \dots, N\} \setminus \{S\}$ having cardinality l . We denote by P_α the probability measures that are associated with uniform traffic.

- Hotspot destination traffic: A given packet is a hotspot destination traffic packet with probability β . For a hotspot destination traffic packet, node N is always a destination. The sending node is chosen uniformly at random among the other nodes $\{1, 2, \dots, N-1\}$. Once sender S is chosen, the fan-out $l \in \{1, 2, \dots, N-1\}$ is chosen at random according to a discrete probability distribution $(\nu_l)_{l=1}^{N-1}$. Once the fan-out l is chosen, a random fan-out subset $\mathcal{F}' \subset (\{1, 2, \dots, N-1\} \setminus \{S\})$ is chosen uniformly at random among all subsets of $\{1, 2, \dots, N-1\} \setminus \{S\}$ having cardinality $(l-1)$, and the fan-out set is $\mathcal{F} = \mathcal{F}' \cup \{N\}$. We denote by Q_β the probability measures that are associated with hotspot destination traffic.
- Hotspot source traffic: A given packet is a hotspot source traffic packet with probability γ . For such a packet, the sending node is chosen to be node N . The fan-out $1 \leq l \leq (N-1)$ is chosen at random according to a discrete probability distribution $(\kappa_l)_{l=1}^{N-1}$. Once the fan-out l is chosen, a random fan-out set $\mathcal{F} \subset \{1, 2, \dots, N-1\}$ is chosen uniformly at random among all subsets of $\{1, 2, \dots, N-1\}$ having cardinality l . We denote by Q_γ the probability measures that are associated with hotspot source traffic.

While our analysis assumes that the traffic type, the source node, the fan-out, and the fan-out set are drawn independently at random, this independence assumption is not critical for the analysis. Our results hold also for traffic patterns displaying correlations, as long as the long run average segment utilizations are equivalent to the utilizations with the independence assumption. For instance, our results hold for a correlated traffic model where a given source node transmits with probability $p < 1$ to exactly the same set of destinations as the previous packet that was sent by the node, and with probability $1-p$ to a new set of destination nodes that were drawn independently at random. We denote by P_α^l the probability measure P_α that is conditioned upon $|\mathcal{F}| = l$ and define Q_β^l and Q_γ^l analogously.

We proceed to take a closer look at the set of active nodes \mathcal{A} containing the sender and all destinations. We order the nodes in this set in increasing order of their indexes, i.e.,

$$\mathcal{A} = \{X_1, X_2, \dots, X_{l+1}\}, \quad 1 \leq X_1 < X_2 < \dots < X_{l+1} \leq N \quad (1)$$

and consider the “gaps”

$$X_1 + (N - X_{l+1}), \quad (X_2 - X_1), \dots, (X_{l+1} - X_l) \quad (2)$$

between successive nodes in the set \mathcal{A} . Observe that l here is the random number of destinations.

For SP routing, i.e., to maximize spatial wavelength reuse, we determine the largest of these gaps. Since there may be a tie among the LGs (in which case, one of the LGs is chosen uniformly at random), we denote the selected LG as “CLG” (for “chosen largest gap”). Suppose that the CLG is between nodes X_{j-1} and X_j . With SP routing, the packet is then sent from sender S to node X_{j-1} and from sender S to node X_j in

the opposite direction. Thus, the CLG is not traversed by the packet transmission.

Let $\mathbb{P}(E)$ denote the overall probability of any event of interest E , so that

$$\mathbb{P}(E) = \alpha \sum_{l=1}^{N-1} P_\alpha^l(E) \cdot \mu_l + \beta \sum_{l=1}^{N-1} Q_\beta^l(E) \cdot \nu_l + \gamma \sum_{l=1}^{N-1} Q_\gamma^l(E) \cdot \kappa_l$$

and note that, by symmetry, $\mathbb{P}\{\hat{u}_1 \text{ is used}\} = \mathbb{P}\{\hat{u}_N \text{ is used}\}$ and $\mathbb{P}\{\hat{u}_1 \text{ is used}\} = \mathbb{P}\{\hat{u}_N \text{ is used}\}$. More generally, for reasons of symmetry, it suffices to compute the utilization probabilities for the clockwise-oriented edges. For $n \in \{1, \dots, N\}$, we abbreviate

$$\hat{n} := \{\hat{u}_n \text{ is used}\}. \quad (3)$$

It will be convenient to identify $0 \equiv N$. We denote by \mathcal{G} , $0 \leq \mathcal{G} \leq N-1$, the (random) node bordering the CLG “from the left” (when this gap is considered clockwise), i.e., \mathcal{G} denotes the lower indexed border node of the CLG. The utilization probability for the clockwise segment n is given by

$$\begin{aligned} \mathbb{P}(\hat{n}) = & \alpha \sum_{l=1}^{N-1} P_\alpha^l(\hat{n}) \cdot \mu_l + \beta \sum_{l=1}^{N-1} Q_\beta^l(\hat{n}) \cdot \nu_l \\ & + \gamma \sum_{l=1}^{N-1} Q_\gamma^l(\hat{n}) \cdot \kappa_l. \end{aligned} \quad (4)$$

Our primary performance metric is the maximum packet throughput (stability limit). More specifically, we define the (effective) multicast capacity C_M as the maximum number of packets (with a given traffic pattern) that can, in the long-run average, be sent simultaneously [39], and note that C_M is given as the reciprocal of the largest ring segment utilization probability, i.e.,

$$C_M := \frac{1}{\max_{n \in \{1, \dots, N\}} \mathbb{P}(\hat{n})}. \quad (5)$$

We note that [39] introduces both a nominal multicast capacity that considers the hop distances that are required to serve multicast packets and an effective multicast capacity that considers the utilization of the ring segments due to the multicast packet transmissions. With the nonuniform traffic that is considered in this paper, the segments of the bidirectional single-wavelength ring are nonuniformly loaded (utilized). The utilization probabilities of the ring segments capture this nonuniform loading, with the most heavily loaded segment limiting the packet throughput. Therefore, we consider the effective multicast capacity, which represents the stability limit of the network, throughout this paper.

III. HOTSPOT MULTICAST CAPACITY FOR SP ROUTING

In this section, we examine the capacity with SP routing, proceeding in three main steps. First, we characterize the ring segment utilization probabilities due to uniform traffic, hotspot

destination traffic, and hotspot source traffic. Second, we evaluate the largest utilization probability, which in turn limits the capacity. Third, we examine the capacity numerically.

A. Characterization of Segment Utilization

1) *Uniform Traffic*: For uniform traffic, we have, for reasons of symmetry, for all $n \in \{1, \dots, N\}$,

$$P_\alpha^l(\hat{n}) = P_\alpha^l(\hat{1}). \quad (6)$$

This probability can be computed according to (17) in [10] as

$$P_\alpha^l(\hat{1}) = \frac{N - g(l, N)}{2N} \quad (7)$$

with the expected length of the LG $g(l, N)$ given by $g(l, N) = \sum_{k=1}^{N-1} k \cdot q_{l,N}(k)$, where $q_{l,N}(\cdot)$ denotes the distribution of the length of the LG. This fundamental distribution may be computed using the recursion

$$q_{l,N}(k) = p_{l,N}(k) \cdot \sum_{m=1}^k q_{l-1,N-k}(m) + \sum_{m=1}^{k-1} p_{l,N}(m) \cdot q_{l-1,N-m}(k) \quad (8)$$

together with the initialization $q_{0,N}(k) = 1$ for $k = N$ and $q_{0,N}(k) = 0$ for $k < N$, where $p_{l,N}(k) = \binom{N-k-1}{l-1} / \binom{N-1}{l}$ denotes the probability that an arbitrary gap has k hops. Note that the distribution of the length of the LG $q_{l,N}(k)$, $k = 1, \dots, N-1$, is the same for all traffic types (uniform traffic, hotspot destination traffic, hotspot source traffic) for a given fixed number of active nodes $(l+1)$ out of the total of N nodes in the network.

2) *Hotspot Destination Traffic*: There are two complementary events that lead to a traversal of the clockwise segment \hat{u}_{n+1} , $n \in \{0, \dots, N-1\}$, leading from node n to node $n+1$: 1) The packet traverses both the clockwise segment \hat{u}_{n+1} and the preceding clockwise segment \hat{u}_n , i.e., the sender is a node $S \neq n$, and 2) node n is the sender ($S = n$) and transmits the packet in the clockwise direction, so that it traverses segment \hat{u}_{n+1} , following node n (in the clockwise direction). Formally

$$Q_\beta^l(n \hat{+} 1) = Q_\beta^l(\hat{n} \text{ and } n \hat{+} 1) + Q_\beta^l(S = n \text{ and } n \hat{+} 1). \quad (9)$$

Next, note that the event that the clockwise segment \hat{u}_n is traversed can be decomposed into two complementary events: 1) Segments \hat{u}_n and \hat{u}_{n+1} are traversed, and 2) segment \hat{u}_n is traversed but not segment \hat{u}_{n+1} , i.e.,

$$Q_\beta^l(\hat{n}) = Q_\beta^l(\hat{n} \text{ and } n \hat{+} 1) + Q_\beta^l(\hat{n} \text{ and not } n \hat{+} 1). \quad (10)$$

Similarly, we can decompose the event of node n being the sender as

$$Q_\beta^l(S = n) = Q_\beta^l(S = n \text{ and } n \hat{+} 1) + Q_\beta^l(S = n \text{ and not } n \hat{+} 1). \quad (11)$$

Hence, we can express $Q_\beta^l(n \hat{+} 1)$ as

$$Q_\beta^l(n \hat{+} 1) = Q_\beta^l(\hat{n}) - Q_\beta^l(\hat{n} \text{ and not } n \hat{+} 1) + Q_\beta^l(S = n) - Q_\beta^l(S = n \text{ and not } n \hat{+} 1). \quad (12)$$

Now, note that there are two complementary events that result in the CLG starting at node n , such that clockwise segment $n+1$ is inside the CLG: 1) Node n is the last destination node reached by the clockwise transmission, i.e., segment n is used, but segment $n+1$ is not used, and 2) node n is the sender and transmits only a packet copy in the counterclockwise direction. Hence

$$Q_\beta^l(\mathcal{G} = n) = Q_\beta^l(\hat{n} \text{ and not } n \hat{+} 1) + Q_\beta^l(S = n \text{ and not } n \hat{+} 1).$$

Therefore

$$Q_\beta^l(n \hat{+} 1) = Q_\beta^l(\hat{n}) + Q_\beta^l(S = n) - Q_\beta^l(\mathcal{G} = n). \quad (13)$$

In particular

$$Q_\beta^l(\hat{1}) = Q_\beta^l(\hat{N}) + Q_\beta^l(S = N) - Q_\beta^l(\mathcal{G} = N). \quad (14)$$

Note that, for hotspot destination traffic, node N is a destination node and, by symmetry, is reached by a clockwise transmission with a probability of $1/2$, i.e.,

$$Q_\beta^l(\hat{N}) = \frac{1}{2}. \quad (15)$$

For hotspot destination traffic, node N cannot be the sender; hence, $Q_\beta^l(S = N) = 0$. The probability for the CLG to start at N (clockwise) is the same as that for the other l gaps (for reasons of symmetry), i.e., $Q_\beta^l(\mathcal{G} = N) = 1/(l+1)$. In summary

$$Q_\beta^l(\hat{1}) = \frac{1}{2} - \frac{1}{l+1}. \quad (16)$$

In Appendix A, we analyze $Q_\beta^l(S = n)$ and $Q_\beta^l(\mathcal{G} = n)$ for $n = 1, \dots, N-1$ to allow for the recursive evaluation of $Q_\beta^l(\hat{n})$ using (13).

3) *Hotspot Source Traffic*: For hotspot source traffic, with node N being the sender, we immediately have

$$Q_\gamma^l(\hat{N}) = 0. \quad (17)$$

For the SP routing policy, the only case where the segment \hat{u}_1 is not used is when the CLG starts directly at the sender node $N \equiv 0$, which occurs with probability $Q_\gamma^l(\mathcal{G} = 0) = 1/(l+1)$.

To see this, note that, with l destinations, there are $l + 1$ gaps, each of which has the same probability to be the CLG (for reasons of symmetry). Hence

$$Q_\gamma^l(\hat{1}) = 1 - Q_\gamma^l(\mathcal{G} = 0) = 1 - \frac{1}{l+1}. \quad (18)$$

Generally, we note that segment $n + 1, n \in \{1, \dots, N - 1\}$, can be utilized only if the preceding segment n is being used (since only node N , which we also refer to as node 0, can be the sender). Hence

$$Q_\gamma^l(n \hat{+} 1) = Q_\gamma^l(\hat{n} \text{ and } n \hat{+} 1) \quad (19)$$

$$= Q_\gamma^l(\hat{n}) - Q_\gamma^l(\hat{n} \text{ and not } n \hat{+} 1) \quad (20)$$

$$= Q_\gamma^l(\hat{n}) - Q_\gamma^l(\mathcal{G} = n) \quad (21)$$

where (20) follows analogously from (10), and (21) follows by noting that the clockwise segment $n + 1$ is not used if and only if the CLG starts at node n (for the considered SP routing with sender node N).

Since $Q_\gamma^l(\mathcal{G} = n)$ only depends on the geometry of the set of active nodes \mathcal{A} , one may compute this probability, as outlined in Appendix A, replacing the β subscripts by γ subscripts. From (21), we see that $Q_\gamma^l(\hat{n})$ is a nonincreasing function of $n \in \{1, \dots, N\}$. Note that the probability $Q_\gamma^l(\mathcal{G} = n)$ is zero for the larger values of n , i.e., for $lN/(l + 1) < n \leq N$, and that $Q_\gamma^l(n \hat{+} 1)$ stabilizes to zero on this interval. To see this, note that, with $l + 1$ active nodes out of N total nodes, the LG must be larger than or equal to $N/(l + 1)$. Hence, the index of the node where the LG starts (in the clockwise sense) must be smaller than or equal to $N - N/(l + 1)$. Consequently, the LG cannot start at a node with an index that is larger than $lN/(l + 1)$.

B. Evaluation of Largest Segment Utilization

In this section, we show that, among all clockwise-oriented edges, \hat{u}_1 or \hat{u}_N has the highest utilization probability. We begin with the following lemma, which is proven in Appendix B.

Lemma 3.1: Letting $x \in \{\beta, \gamma\}$ and fixing a fan-out cardinality $l, 1 \leq l \leq N - 1$, one has, for all $n \in \{1, \dots, N - 1\}$, the following:

$$Q_x^l(\mathcal{G} = n | \mathcal{G} \geq n) \geq \frac{1}{N - n}.$$

With this lemma, we can show the main statement.

Theorem 3.2: Among all clockwise-oriented edges, \hat{u}_1 or \hat{u}_N has the highest probability to be used, and this maximal probability can be expressed as

$$\begin{aligned} \max_{n \in \{1, \dots, N\}} \mathbb{P}(\hat{n}) &= \alpha P_\alpha(\hat{1}) + \frac{\beta}{2} \\ &+ \max \left\{ -\beta \sum_{l=1}^{N-1} \frac{\nu_l}{l+1} + \gamma \left(1 - \sum_{l=1}^{N-1} \frac{\kappa_l}{l+1} \right), 0 \right\}. \end{aligned}$$

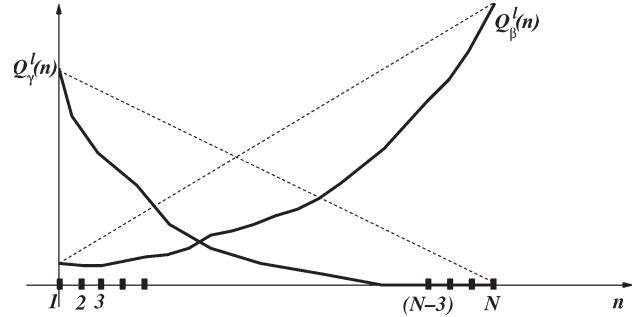


Fig. 2. Chords used in the proof of Theorem 3.2.

Proof: First, viewing $Q_\beta^l(\hat{n})$ and $Q_\gamma^l(\hat{n})$ as functions of $n \in \{1, \dots, N\}$, it suffices to verify that these functions have their values lying beneath the chords connecting their endpoints at 1 and N (see Fig. 2).

Consider the case γ : Since $Q_\gamma^l(\hat{N}) = 0$, we have to show

$$Q_\gamma^l(\hat{n}) \leq Q_\gamma^l(\hat{1}) \frac{N - n}{N - 1}. \quad (22)$$

Using a telescopic expansion, we see that this is fulfilled as soon as

$$\frac{Q_\gamma^l(m \hat{+} 1)}{Q_\gamma^l(\hat{m})} \leq 1 - \frac{1}{N - m} \quad \forall m \in \{1, \dots, N - 1\}. \quad (23)$$

Since m is not the sender, we have

$$\begin{aligned} \frac{Q_\gamma^l(m \hat{+} 1)}{Q_\gamma^l(\hat{m})} &= \frac{Q_\gamma^l(m \hat{+} 1 \text{ and } \hat{m})}{Q_\gamma^l(\hat{m})} \\ &= Q_\gamma^l(m \hat{+} 1 | \hat{m}). \end{aligned} \quad (24)$$

The probability of the complementary event is

$$\begin{aligned} Q_\gamma^l(\text{not } m \hat{+} 1 | \hat{m}) &= Q_\gamma^l(\mathcal{G} = m | \hat{m}) \\ &= Q_\gamma^l(\mathcal{G} = m | \mathcal{G} \geq m). \end{aligned} \quad (25)$$

Hence, it remains to be shown that

$$Q_\gamma^l(\mathcal{G} = m | \mathcal{G} \geq m) \geq \frac{1}{N - m} \quad (26)$$

but this is exactly the statement of Lemma 3.1.

Next, consider case β : Here, one has to show that

$$Q_\beta^l(\hat{n}) \leq Q_\beta^l(\hat{0}) + (Q_\beta^l(\hat{1}) - Q_\beta^l(\hat{0})) \frac{N - n}{N - 1} \quad \forall n \in \{1, \dots, N\}. \quad (27)$$

We use (14) and obtain, since N is not a sender:

$$Q_\beta^l(\hat{1}) - Q_\beta^l(\hat{0}) = -Q_\beta^l(\mathcal{G} = 0). \quad (28)$$

Moreover

$$\begin{aligned} Q_{\beta}^l(\hat{n}) - Q_{\beta}^l(\hat{0}) &= \sum_{m=n}^{N-1} Q_{\beta}^l(\hat{m}) - Q_{\beta}^l(m \hat{+} 1) \\ &= \sum_{m=n}^{N-1} (Q_{\beta}^l(\mathcal{G} = m) - Q_{\beta}^l(S = m)) \\ &= Q_{\beta}^l(\mathcal{G} \geq n) - \frac{N-n}{N-1}. \end{aligned} \quad (29)$$

The last equality holds since, for reasons of symmetry, $Q_{\beta}^l(S = m) = 1/(N-1)$. So, we now know that inequality (27) is equivalent to

$$Q_{\beta}^l(\mathcal{G} \geq n) \leq \frac{N-n}{N-1} (1 - Q_{\beta}^l(\mathcal{G} = 0)) \quad \forall n \in \{1, \dots, N\}. \quad (30)$$

We now use

$$1 - Q_{\beta}^l(\mathcal{G} = 0) = Q_{\beta}^l(\mathcal{G} \geq 1) \quad (31)$$

and see that (30) is satisfied if, for all $m \in \{1, \dots, N-1\}$

$$\frac{Q_{\beta}^l(\mathcal{G} \geq m+1)}{Q_{\beta}^l(\mathcal{G} \geq m)} \leq 1 - \frac{1}{N-m}. \quad (32)$$

This is directly equivalent to

$$\frac{Q_{\beta}^l(\mathcal{G} = m)}{Q_{\beta}^l(\mathcal{G} \geq m)} \geq \frac{1}{N-m} \quad (33)$$

and we can again apply Lemma 3.1.

Let us recall that

$$\mathbb{P}(\hat{n}) = \alpha P_{\alpha}(\hat{n}) + \beta Q_{\beta}(\hat{n}) + \gamma Q_{\gamma}(\hat{n}). \quad (34)$$

Therefore

$$\mathbb{P}(\hat{n}) = \sum_{l=1}^{N-1} (\alpha \mu_l P_{\alpha}^l(\hat{n}) + \beta \nu_l Q_{\beta}^l(\hat{n}) + \gamma \kappa_l Q_{\gamma}^l(\hat{n})). \quad (35)$$

Thus, the function $n \mapsto \mathbb{P}(n)$ is a convex combination of $n \mapsto P_{\alpha}^l(\hat{n})$, $n \mapsto Q_{\beta}^l(\hat{n})$, and $n \mapsto Q_{\gamma}^l(\hat{n})$, and as such, $n \mapsto \mathbb{P}(n)$ also has to have a graph lying below the chord connecting its endpoints. As a consequence, the maximum value $\max_{1 \leq n \leq N} \mathbb{P}(\hat{n})$ must be attained at the boundary of the discrete interval $\{1, 2, \dots, N\}$, i.e.,

$$\max_{n \in \{1, \dots, N\}} \mathbb{P}(\hat{n}) = \max \left\{ \mathbb{P}(\hat{1}), \mathbb{P}(\hat{N}) \right\}. \quad (36)$$

This maximum can be evaluated by inserting the values (15)–(18) into the representation (35) and use (6), so that

$$\begin{aligned} \max_{n \in \{1, \dots, N\}} \mathbb{P}(\hat{n}) &= \alpha P_{\alpha}(\hat{1}) + \frac{\beta}{2} \\ &+ \max \left\{ -\beta \sum_{l=1}^{N-1} \frac{\nu_l}{l+1} + \gamma \left(1 - \sum_{l=1}^{N-1} \frac{\kappa_l}{l+1} \right), 0 \right\} \end{aligned} \quad (37)$$

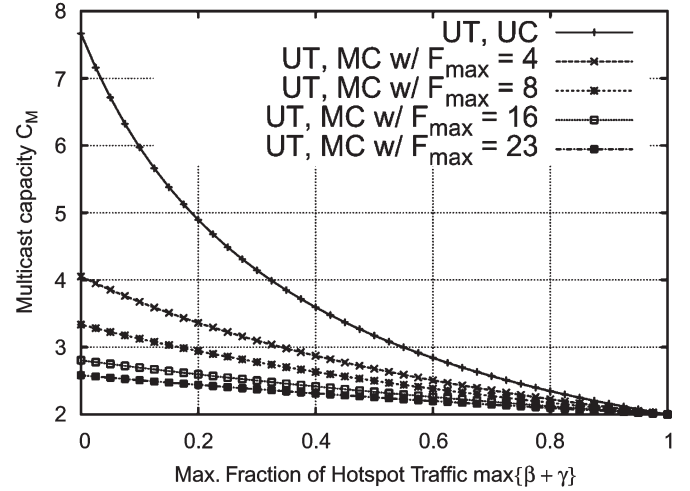


Fig. 3. Multicast capacity C_M as a function of the maximum fraction of hotspot traffic $\max\{\beta, \gamma\}$, whereby all hotspot traffic is unicast. Uniform traffic (UT) ranges from unicast (UC) to multicast (MC) with different maximum fan-out F_{\max} . Number of nodes: $N = 24$.

for all traffic portions α , β , and γ , and fan-out distributions $(\mu_l)_{l=1}^{N-1}$, $(\nu_l)_{l=1}^{N-1}$, and $(\kappa_l)_{l=1}^{N-1}$. \square

C. Numerical Evaluation

In this section, we numerically examine the multicast capacity that is achieved with SP routing. In Fig. 3, we consider uniform traffic ranging from unicast with $\mu_1 = 1$ and $\mu_l = 0$ for $l = 2, \dots, N-1$ to multicast with different maximum fan-outs, whereby $\mu_l = 1/(F_{\max} - 1)$ for $l = 2, \dots, F_{\max}$ and $\mu_l = 0$ for $l = F_{\max} + 1, \dots, N-1$, mixed with a maximum fraction $\max\{\beta, \gamma\}$ of unicast ($\nu_1 = 1, \kappa_1 = 1$, and $\nu_l = \kappa_l = 0$ for $l = 2, \dots, N-1$) hotspot traffic. Note that, for unicast hotspot traffic, (37) reduces to $\max_{n \in \{1, \dots, N\}} \mathbb{P}(\hat{n}) = \alpha P_{\alpha}(\hat{1}) + (1/2) \max\{\beta, \gamma\}$. Thus, for unicast hotspot traffic, only the larger of the portion of hotspot destination traffic β and the portion of hotspot source traffic γ influences the multicast capacity, as illustrated in Fig. 3. The curves in the figure are obtained by setting $\gamma = 0$ and increasing β from 0 to 1 (while α decreases from 1 to 0).

In Fig. 4, we plot the multicast capacity when all traffic is multicast with a maximum fan-out $F_{\max} = 16$ as a function of the total fraction of hotspot traffic $\beta + \gamma$. We consider different hotspot traffic mixes. The scenario where all hotspot traffic is hotspot destination traffic (i.e., $\gamma = 0$) gives the largest capacity for this moderately large fan-out since including the hotspot in the already moderately large fan-out set is a relatively small change from reaching destinations in a uniformly distributed fan-out set of this size. As the portion of hotspot source traffic γ increases to the point where all hotspot traffic is hotspot source traffic (i.e., $\beta = 0$), the capacity drops quite significantly, particularly, for large total portions of hotspot traffic $\beta + \gamma$ that are close to one. Intuitively, a given hotspot source traffic packet requires the sending of a packet copy in both ring directions, unless the CLG is adjacent to the hotspot. With increasing fan-out, it becomes less likely that the CLG is adjacent to the hotspot. In the broadcast traffic case ($\kappa_{N-1} = 1$), the CLG

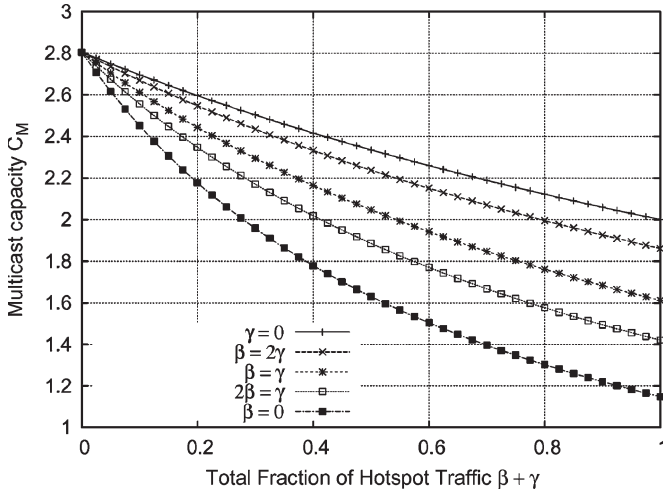


Fig. 4. Multicast capacity C_M as a function of the total fraction of hotspot traffic $\beta + \gamma$ for different compositions of hotspot traffic from only hotspot destination traffic ($\gamma = 0$) to only hotspot source traffic ($\beta = 0$). All traffic is multicast with maximum fan-out $F_{\max} = 16$. $N = 24$.

is adjacent to the hotspot with probability $2/N$; hence, the segment \hat{u}_1 is used for each hotspot source traffic packet with probability $1 - 1/N$. (Similarly, the segment \hat{u}_N is used with probability $1 - 1/N$.) As a result, the multicast capacity drops to close to one when SP routing is employed, for a traffic mix with a large portion of hotspot source traffic having a moderately large to large fan-out.

IV. HOTSPOT MULTICAST CAPACITY WITH SP/OC ROUTING

In this section, we propose a novel routing strategy that avoids the high utilization of the segments \hat{u}_1 and \hat{u}_N for hotspot source traffic and the resulting reduction in the multicast capacity. First, in Section IV-A, we introduce and analyze an OC routing strategy that utilizes only one of the segments, i.e., either segment \hat{u}_1 or segment \hat{u}_N , but not both for sending hotspot source traffic. Next, in Section IV-B, we combine the SP and OC routing strategies.

A. OC Routing: Definition and Analysis

We define the OC routing strategy as follows: Given that the hotspot node N is the sender, let X_1 denote the lowest indexed destination node (i.e., the first destination node encountered clockwise), and let X_l denote the highest indexed destination node (i.e., the last destination node encountered clockwise before $X_{l+1} = N$). If $X_1 > N - X_l$, then the packet is sent in the counterclockwise direction from node N to node X_1 . On the other hand, if $N - X_l > X_1$, then the packet is sent in the clockwise direction from node N to node X_l . Ties are broken symmetrically. Intuitively, with this OC strategy, node N sends only *one* copy of the packet in the ring direction that reaches all destination nodes with the smallest hop count. Note that this OC strategy does not minimize, in general, the hop count: If $\max\{X_1, N - X_l\}$ is as large as the CLG, then the OC strategy achieves the minimum hop count. If $\max\{X_1, N - X_l\}$ is

smaller than the CLG, then the OC strategy incurs a larger hop count than SP routing and consequently does not maximize spatial wavelength reuse. However, when employed judiciously for the hotspot source traffic, this OC strategy can lead to significant increases in the multicast capacity over SP routing. Traffic from the regular nodes is routed with the SP strategy throughout. In summary, we define the *OC routing* strategy as employing OC routing for the hotspot source traffic and SP routing for the uniform and hotspot destination traffic. We denote by \tilde{Q}_γ and $\tilde{\mathbb{P}}$ the probability measures that are associated with OC routed hotspot source traffic.

As we illustrate in Section IV-C, the segments \hat{u}_1 or \hat{u}_N are no longer guaranteed to attain the maximum utilization when the OC routing strategy is employed. To assess the multicast capacity with OC routing, we analyze therefore the segment utilization probabilities $\tilde{Q}_\gamma^l(\hat{n})$, $n = 1, \dots, N$, due to OC routed hotspot source traffic. Together with the utilization probabilities $Q_\beta^l(\hat{n})$ (as analyzed in Appendix A) due to SP routed hotspot destination traffic and $P_\alpha^l(\hat{n})$ [given in (7)] due to SP routed uniform traffic, the utilization probabilities $\tilde{Q}_\gamma^l(\hat{n})$ can be used in (4) to evaluate the total segment utilization probabilities $\tilde{\mathbb{P}}(\hat{n})$ and, subsequently, the multicast capacity C_M using (5).

For the evaluation of $\tilde{Q}_\gamma^l(\hat{n})$, $n = 1, \dots, N$, we first note that $\tilde{Q}_\gamma^l(\hat{1}) = 1/2$, whereas $\tilde{Q}_\gamma^l(\hat{N}) = 0$. Then, for intermediate segments \hat{u}_n , $2 \leq n \leq N - 1$, we have

$$\tilde{Q}_\gamma^l(\hat{n}) = \tilde{Q}_\gamma^l(n \hat{-} 1) - \tilde{Q}_\gamma^l(X_l = n - 1, n \hat{-} 1) \quad (38)$$

since a packet traversing segment u_{n-1} also traverses segment \hat{u}_n , unless node $n - 1$ is the last destination node in the clockwise direction. Moreover

$$\begin{aligned} \tilde{Q}_\gamma^l(X_l = n - 1, n \hat{-} 1) &= \sum_{j=1}^{(N-n) \wedge (n-1)} \tilde{Q}_\gamma^l(X_l = n - 1, X_1 = j) \\ &+ \frac{1}{2} \tilde{Q}_\gamma^l(X_l = n - 1, X_1 = N - n + 1) \end{aligned} \quad (39)$$

since the packet is routed clockwise to the last destination node $X_l = n - 1$ if $X_1 < N - X_l$, i.e., if $X_1 \leq N - n$, to avoid the LG neighboring the source node. In case of a tie, i.e., if $X_1 = N - n + 1$, then the packet is routed clockwise with a probability of $1/2$. Observe that the joint probabilities $\tilde{Q}_\gamma^l(X_l = a, X_1 = b)$ are given by

$$\tilde{Q}_\gamma^l(X_l = a, X_1 = b) = \binom{a-b-1}{l-2} / \binom{N-1}{l} \quad (40)$$

where $a \geq (b + l - 1)$. Introducing the Heaviside (unit step) function

$$H(x) = \begin{cases} 1, & \text{if } x \geq 0 \\ 0, & \text{if } x < 0 \end{cases} \quad (41)$$

and using the following identity for binomial coefficients:

$$\sum_{n=M_1}^{M_2} \binom{n}{k} = \binom{M_2+1}{k+1} - \binom{M_1}{k+1} \quad (42)$$

that is valid for $k \leq M_1 < M_2$, we obtain the following recursion for $2 \leq n \leq N-1$:

$$\begin{aligned} \tilde{Q}_\gamma^l(\hat{n}) &= \tilde{Q}_\gamma^l(n \hat{-} 1) \\ &\quad - \left[\binom{n-2}{l-1} H(n-l-1) \right. \\ &\quad \left. - \left(\binom{2n-N-2}{l-1} - \frac{1}{2} \binom{2n-N-3}{l-2} \right) \right] \\ &\quad \times H(2n-N-1-l) \Big/ \binom{N-1}{l}. \quad (43) \end{aligned}$$

Noting that, for all segments \hat{u}_n , $n=1, \dots, N$, we have $Q_\beta^l(\hat{n}) \leq Q_\beta^l(\hat{N}) = 1/2$ for the utilization due to SP routed hotspot destination traffic and $\tilde{Q}_\gamma^l(\hat{n}) \leq \tilde{Q}_\gamma^l(\hat{1}) = 1/2$ for the utilization due to OC routed hotspot source traffic, we have

$$\max_{n \in \{1, \dots, N\}} \tilde{\mathbb{P}}(\hat{n}) \leq \alpha P_\alpha(\hat{1}) + \frac{1}{2}(\beta + \gamma) \quad (44)$$

as an upper bound on the total segment utilization with the OC routing strategy. A lower bound on the multicast capacity C_M with the OC routing strategy is thus given by

$$C_M \geq \frac{1}{\alpha P_\alpha(\hat{1}) + \frac{1}{2}(\beta + \gamma)}. \quad (45)$$

On the other hand, noting that, with OC routing, the utilization probability of segment \hat{u}_1 due to hotspot source traffic is reduced to $\tilde{\mathbb{P}}_\gamma^l(\hat{1}) = 1/2$, we have the lower bound on the total segment utilization

$$\begin{aligned} \max_{n \in \{1, \dots, N\}} \tilde{\mathbb{P}}(\hat{n}) &\geq \max \left\{ \tilde{\mathbb{P}}(\hat{1}), \tilde{\mathbb{P}}(\hat{N}) \right\} \\ &= \alpha P_\alpha(\hat{1}) + \frac{\beta}{2} + \max \left\{ -\beta \sum_{l=1}^{N-1} \frac{\nu_l}{l+1} + \frac{\gamma}{2}, 0 \right\}. \quad (46) \end{aligned}$$

Note that the lower bound (46) on the segment utilization with the OC routing strategy is less than or equal to the utilization (37) with SP routing for all traffic types. Consequently, the upper bound on the multicast capacity with the OC routing strategy that is given by the reciprocal of (46) is larger or equal to the multicast capacity that is given by the reciprocal of (37).

We assumed throughout this section that the hotspot node distinguishes between a packet that it generated as unicast traffic (and routed according to SP routing) and a packet that is generated as hotspot source traffic (and routed according to OC routing). It may be more practical to apply the OC strategy to any packet with node N as the source node, irrespective of whether the packet corresponds to uniform traffic (and just happened to selected node N as the random source node) or

to hotspot source traffic. This would effectively result in a portion $\alpha(1-1/N)$ of uniform traffic and a portion $\gamma + \alpha/N$ of hotspot source traffic. The segment utilization probabilities due to uniform and hotspot source traffic would be unchanged from the preceding expressions, but the traffic proportions that were used in evaluating (4) would need to be adjusted by α/N , as outlined. The effect of this adjustment quickly diminishes with the number of nodes N , and we continue to assume that the hotspot node can distinguish between the uniform and hotspot source traffic packets in the remainder of this paper.

B. Combined SP/OC Routing Strategy

As readily seen from Theorem 3.2, the hotspot source traffic does not affect the maximum segment utilization with SP routing (for all traffic types) as long as

$$\gamma \leq \frac{\beta \sum_{l=1}^{N-1} \frac{\nu_l}{l+1}}{1 - \sum_{l=1}^{N-1} \frac{\kappa_l}{l+1}} =: \gamma_{\text{th1}} \quad (47)$$

because then the maximum utilization is attained at $\alpha P_\alpha(\hat{1}) + (\beta/2)$. Intuitively, the fulfillment of (47) corresponds to N being primarily a ‘‘Receiving Hotspot.’’

As the portion of hotspot source traffic γ increases above the threshold γ_{th1} , i.e., as N becomes primarily a ‘‘Sending Hotspot,’’ the multicast capacity may be increased by employing the OC routing strategy from the preceding section. The lower bound of the multicast capacity with the OC routing strategy (45) exceeds the multicast capacity with SP routing, which was obtained as the reciprocal of (37) when the portion of hotspot source traffic γ becomes so large that

$$\gamma > \frac{\beta \sum_{l=1}^{N-1} \frac{\nu_l}{l+1}}{\frac{1}{2} - \sum_{l=1}^{N-1} \frac{\kappa_l}{l+1}} =: \gamma_{\text{th2}}. \quad (48)$$

Thus, when inequality (48) is fulfilled, we are guaranteed to achieve a larger multicast capacity with the OC routing strategy than with SP routing.

Based on these threshold criteria, we define the *combined SP/OC routing* strategy as follows: The hotspot periodically estimates the current traffic parameters, i.e., the traffic portions α , β , and γ as well as the corresponding fan-out distributions μ_l , ν_l , and κ_l , $l=1, \dots, N-1$. These traffic estimates may be based on a combination of traffic measurements and historic traffic patterns, using techniques that are similar to those in [58]–[62]. From the traffic parameters, the hotspot evaluates the thresholds γ_{th1} and γ_{th2} , as given in (47) and (48). The critical threshold $\gamma_{\text{th_crit}}$, i.e., the ‘‘crossover’’ point from higher capacity with SP routing to higher capacity with OC routing, is contained in the interval $[\gamma_{\text{th1}}, \gamma_{\text{th2}}]$. To find the crossover point, the hotspot evaluates the multicast capacity C_M for SP routing using (37) and for OC routing using the methodology that was provided in Section IV-A and finds the crossover point of these two capacities with standard numerical methods, e.g., bisection, in the interval $[\gamma_{\text{th1}}, \gamma_{\text{th2}}]$. If the fraction of hotspot

source traffic $\gamma \leq \gamma_{th_crit}$, then SP routing is employed for all traffic. On the other hand, if $\gamma \geq \gamma_{th_crit}$, then the OC routing strategy is employed, i.e., the hotspot sends its hotspot source traffic (or all of its traffic) using OC routing, while all other nodes send their traffic using SP routing.

C. Numerical Results

In this section, we numerically examine the multicast capacity C_M of the SP and OC routing strategies, as well as the combined SP/OC strategy. Before we examine in detail the multicast capacities for the different routing strategies, we briefly provide insight into the relevance of the proposed OC routing strategy by examining inequality (48) for illustrative traffic scenarios. Consider a traffic scenario with a portion β of unicast hotspot destination traffic, i.e., $\nu_1 = 1$. Then, the OC routing strategy is guaranteed to achieve a larger multicast capacity than the SP routing strategy when $\gamma > \gamma_{th2} = \beta / (1 - 2 \sum_{l=1}^{N-1} (\kappa_l / (l + 1)))$. For hotspot source multicast traffic with equal portions of one, two, or three receivers, i.e., $\kappa_1 = \kappa_2 = \kappa_3 = 1/3$, we obtain $\gamma_{th2} = 3.6\beta$, whereas for hotspot source traffic with equal portions of up to eight receivers, i.e., $\kappa_1 = \dots = \kappa_8 = 1/8$, we obtain $\gamma_{th2} \approx 1.842\beta$. Thus, we observe that the OC routing strategy becomes relevant for such a basic traffic scenario with unicast hotspot destination traffic as soon as the fraction of hotspot source traffic exceeds the fraction of hotspot destination traffic by relatively small constants, which is likely to occur in practice due to IPTV and similar applications distributing large traffic amounts from a hotspot. In addition, observe that, for the case of only uniform and hotspot source traffic, i.e., $\beta = 0$, the OC routing strategy provides higher capacity for any nonzero portion of hotspot source multicast traffic.

Throughout the following investigations, we plot the multicast capacity C_M as a function of the fraction of hotspot source traffic γ . We illustrate the impact of the fraction of hotspot destination traffic β , the fan-out of the hotspot source traffic (controlled by the distribution $\kappa_l, l = 1, \dots, N - 1$), and the fan-out of the hotspot destination traffic (controlled by the distribution $\nu_l, l = 1, \dots, N - 1$) in Figs. 5–7, respectively. For each traffic scenario, we report the corresponding thresholds γ_{th1} and γ_{th2} in the figures.

We first observe from the figures that, as expected, an increasing fraction of hotspot destination traffic β and increasing fan-out (achieved here by setting $\nu_d = 1$ or $\kappa_d = 1$ for increasing d with all $\nu_l, \kappa_l = 0$ for $l \neq d$) result in smaller multicast capacity. Importantly, we observe that the multicast capacity with OC routing never drops below two, whereas the multicast capacity with SP routing can drop well below two.

For the traffic scenarios considered in Fig. 5, the γ thresholds are close to zero. OC routing gives the same capacity as SP routing for the small range $0 \leq \gamma \leq \gamma_{th1}$ and larger capacity for the range $\gamma > \gamma_{th1}$. Similarly, we observe for the smaller fan-out scenarios $\kappa_2 = 1$ and $\kappa_8 = 1$ in Fig. 6 that SP routing and OC routing give the same capacity in the range $0 \leq \gamma \leq \gamma_{th1}$, whereby the threshold γ_{th1} is significantly larger in the examples in Fig. 6. For these $\kappa_2 = 1$ and $\kappa_8 = 1$ scenarios in Fig. 6, OC routing achieves larger capacities than SP routing as soon as $\gamma > \gamma_{th1}$.

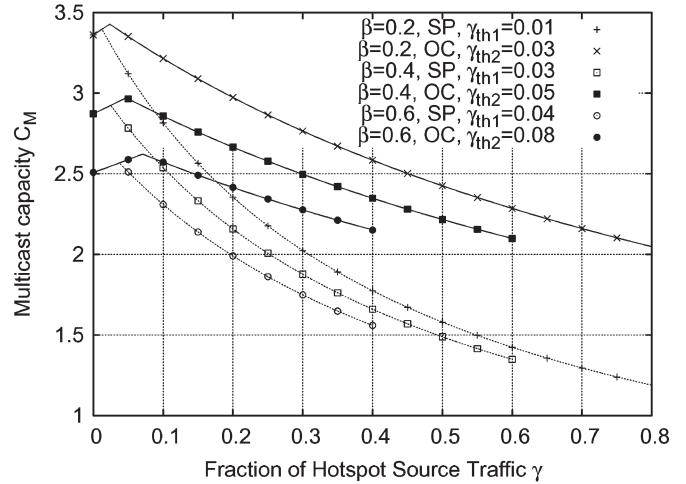


Fig. 5. Multicast capacity C_M as a function of the fraction of hotspot source traffic γ for different fractions of hotspot destination traffic β . Uniform traffic is multicast (MC) with maximum fan-out $F_{max} = 4$; hotspot destination and source traffic are multicast with 16 receivers, i.e., $\nu_{16} = \kappa_{16} = 1$. Number of nodes $N = 24$.

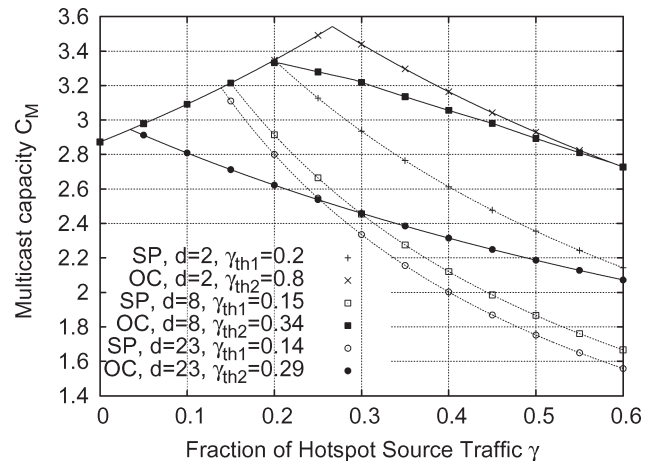


Fig. 6. Multicast capacity C_M as a function of the fraction of hotspot source traffic γ for different fan-outs of hotspot source traffic $\kappa_d = 1$ (uniform traffic with $F_{max} = 4$, hotspot destination traffic with $\beta = 0.4, \nu_2 = 1$, and $N = 24$).

In contrast, in the larger fan-out example $\kappa_{23} = 1$ in Fig. 6, SP routing achieves larger multicast capacity than OC routing for small fractions γ of hotspot source traffic, and the “crossover” from higher capacity with SP routing to higher capacity with OC routing is toward the upper end of the $[\gamma_{th1}, \gamma_{th2}]$ interval.

Turning to Fig. 7, we observe that, for small hotspot destination traffic fan-outs $\nu_1 = 1$ and $\nu_2 = 1$, as well as for large fan-out $\nu_{23} = 1$, the behavior is similar to the large hotspot source traffic fan-out ($\kappa_{23} = 1$) in Fig. 6 in that SP routing achieves higher capacity for small γ ; then, for a critical fraction of hotspot source traffic γ that is close to the middle of the interval $[\gamma_{th1}, \gamma_{th2}]$, there is a crossover to higher capacity with OC routing. (The curves for (OC, $d = 1$) and (OC, $d = 2$) are indistinguishable in the figure.) For the moderately large hotspot source traffic fan-out $\kappa_{16} = 1$ in Fig. 7, the dynamics are similar to the small hotspot source traffic examples in Fig. 6,

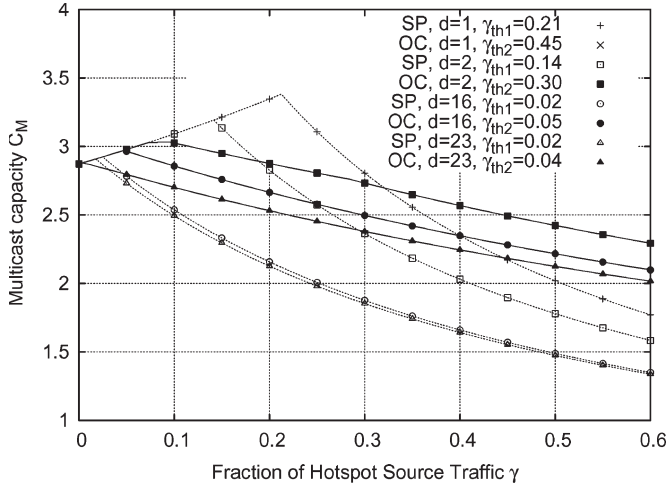


Fig. 7. Multicast capacity C_M as a function of the fraction of hotspot source traffic γ for different fan-outs of hotspot destination traffic $\nu_d = 1$ (uniform traffic with $F_{\max} = 4$, $\beta = 0.4$, hotspot source traffic with $\kappa_{16} = 1$, and $N = 24$).

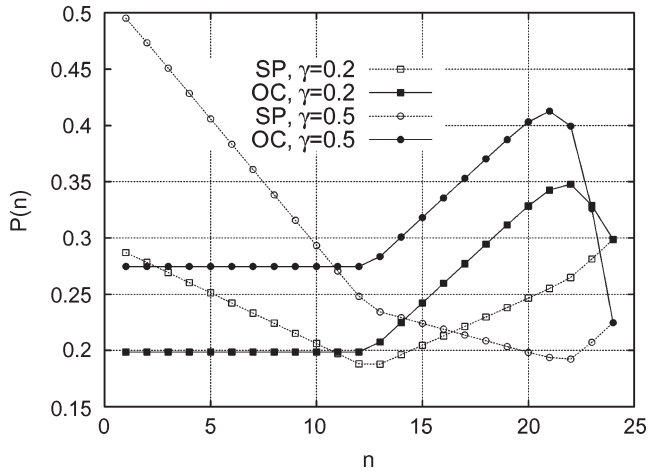


Fig. 8. Segment utilization probability with SP routing $\mathbb{P}(\hat{n})$ and with OC strategy $\tilde{\mathbb{P}}(\hat{n})$ as a function of segment index n for different γ (uniform traffic with $F_{\max} = 4$, $\beta = 0.4$, $\nu_1 = 1$, $\kappa_{16} = 1$, and $N = 24$).

with OC routing achieving the same capacity as SP routing for small γ and then larger capacity for γ larger than γ_{th1} .

In Fig. 8, we plot the segment utilization probabilities $\mathbb{P}(\hat{n})$ and $\tilde{\mathbb{P}}(\hat{n})$ with SP and OC routing, respectively, for the example with $\nu_1 = 1$ (i.e., $d = 1$) in Fig. 7. Specifically, we plot the segment utilizations for $\gamma = 0.2$ where SP routing achieves a capacity of 3.35 compared to 2.88 with OC routing and for $\gamma = 0.5$ where OC routing achieves a capacity of 2.42 compared to 2.02 with SP routing. This example clearly demonstrates that, with OC routing, the segments \hat{u}_1 and \hat{u}_N do not attain the maximum utilization, whereas with SP routing, one of these segments is guaranteed to attain the maximum utilization, as proven in Theorem 3.2 and illustrated in Fig. 8. For a large fraction of hotspot source traffic γ , OC routing achieves overall a more uniform loading of the segments and thus higher capacity.

An analysis of the segment utilization probabilities, as depicted in Fig. 8, can help in identifying the “bottleneck” segments and in guiding evolutionary network upgrades to relieve those bottlenecks. More specifically, for the most common traffic patterns and the corresponding preferable routing strategies, the segment utilizations can be evaluated with our analytical results. The most heavily loaded bottleneck segments can then be upgraded by employing a second wavelength on these segments (using two transmitters and receivers in the nodes bordering on these segments). By equally splitting the traffic over the two wavelength channels of the upgraded segments, their utilization is approximately half of the utilization before the upgrade. The other (nonupgraded) segments continue to operate as before, and the next most heavily utilized segment becomes the new bottleneck limiting the capacity.

Overall, these numerical examples illustrate that, in general, there is a critical threshold for hotspot source traffic: Below the threshold, SP routing achieves higher (or the same) capacity as OC routing, whereas above the threshold, OC routing achieves higher capacity. Our combined SP/OC routing policy outlined in Section IV-B achieves the higher of the two capacities across the entire range of the fraction of hotspot source traffic by adaptively switching between SP and OC routing at the critical threshold.

D. Simulation Results

In this section, we present simulation results that complement the numerical results that were obtained from our capacity analysis. We simulated a bidirectional single-wavelength ring network connecting $N = 24$ nodes. The ring had a circumference of 100 km, a propagation speed of $2 \cdot 10^8$ m/s, and a transmission rate of 1 Gb/s. We consider Poissonian packet generation with a typical trimodal packet size distribution of 50% 40-B packets, 30% 552-B packets, and 20% 1500-B packets. Each node had unlimited station buffers for the generated packets. Each intermediate node forwarding a packet along the ring performed optical–electrical–optical conversion, i.e., the packet incurred a transmission delay at each intermediate node. Intermediate nodes gave priority to forwarding packets on the ring. Thus, no generated packet was lost. We examine the mean aggregate multicast throughput, which is defined as the mean number of simultaneous multicast transmissions in the long-run average and is bounded from above by the analyzed multicast capacity C_M . We also examine the mean packet delay from packet generation until the complete reception of the last copy of the packet by the last destination node, i.e., until the packet has been delivered to all of its destinations. We measure the mean packet delay in terms of the propagation round-trip time of the ring, i.e., 1 ms.

In Fig. 9, we plot the mean packet delay as a function of the mean aggregate multicast throughput for the scenario that was considered in Fig. 6 with a fraction $\gamma = 0.4$ of hotspot source traffic with $d = 8$ destinations. The curves from left to right are obtained by increasing the traffic generation rate and give the 95% confidence intervals for both delay and throughput. We observe that the mean aggregate multicast throughput approaches the multicast capacities C_M that were obtained with

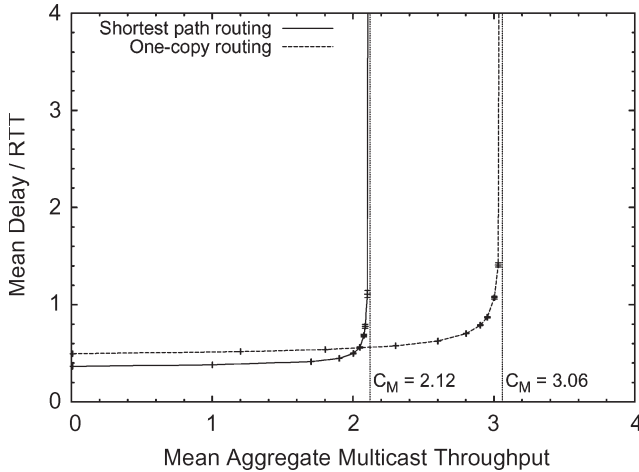


Fig. 9. Mean packet delay as a function of mean aggregate multicast throughput for the scenario that was examined in Fig. 6 with $d = 8$ and $\gamma = 0.4$. For both SP routing and OC routing, the packet delay grows very large as the multicast throughput approaches the multicast capacity C_M .

our analysis for both the SP and OC routing strategies, thus verifying the analysis. We also observe that, for low loads, SP routing gives somewhat lower delays. This is because the typically two packet copies that are sent for hotspot source traffic with SP routing travel shorter distances around the ring to reach their respective destination nodes. With OC routing of hotspot source traffic, a single packet copy is used to reach all destinations, resulting in typically longer distances that are traveled by the single packet copy. Importantly, we observe that the proposed OC routing strategy achieves significantly larger multicast throughputs than the SP routing strategy, as predicted by our multicast capacity analysis.

V. CONCLUSION

We have examined the capacity (maximum achievable long-run average throughput) of a bidirectional optical packet ring with a hotspot for an arbitrary mix of unicast, multicast, and broadcast traffic. We have found that the commonly employed SP routing policy, which achieves the largest capacity for uniform traffic, leads to significant capacity reductions when the portion of multicast traffic originating at the hotspot (hotspot source traffic) exceeds a critical threshold. We have proposed a combined SP/OC routing policy that routes all traffic using SP routing when the hotspot source traffic is below the threshold and routes traffic originating at the hotspot using an OC routing policy and the other traffic using SP routing when the hotspot source traffic is above the threshold.

There are several important directions for future work. One direction is to expand the capacity and routing evaluations that were reported here for single-wavelength bidirectional optical packet rings to WDM rings with multiple wavelength channels in each ring direction, possibly with multiple transceivers at the hotspot, or stacks of WDM rings [63]. Another direction is to examine the capacity and optimal routing for hotspot traffic in ring networks that are meshed with a hub, e.g., [64] and [65], which have so far only been analyzed for uniform traffic.

APPENDIX A

ANALYSIS OF $Q_\beta^l(S = n)$ AND $Q_\beta^l(\mathcal{G} = n)$

For $Q_\beta^l(S = n)$, one simply has

$$Q_\beta^l(S = n) = \frac{1}{N-1} \quad \forall n \in \{1, 2, \dots, N-1\}. \quad (\text{A.1})$$

In order to evaluate $Q_\beta^l(\mathcal{G} = n)$, we proceed as follows: First, for reasons of symmetry, we obtain

$$Q_\beta^l(\mathcal{G} = N) = \frac{1}{l+1}. \quad (\text{A.2})$$

Assume now that $1 \leq n < N$. In order to evaluate $Q_\beta^l(\mathcal{G} = n)$, we first give a recursive formula for the probability that the CLG has length k and that there are m LGs (of length k) along the ring. For $m \geq 2$, we compute this probability recursively as

$$\begin{aligned} Q_\beta^{N,l}(|\text{CLG}| = k, \#(\text{LG}) = m) &= Q_\beta^{N,l}(X_1 = k) \cdot Q_\beta^{N-k,l-1}(|\text{CLG}| = k, \#(\text{LG}) = m-1) \\ &+ \sum_{i=1}^{k-1} Q_\beta^{N,l}(X_1 = i) \cdot Q_\beta^{N-i,l-1}(|\text{CLG}| = k, \#(\text{LG}) = m) \end{aligned} \quad (\text{A.3})$$

whereby the second term on the right-hand side (RHS) corresponds to a “merging” of the first nodes in the network, yielding a smaller ring.

The case $m = 1$ needs to be treated separately by replacing, for $m = 1$, the (rather nonsensical) probability

$$Q_\beta^{N-k,l-1}(|\text{CLG}| = k, \#(\text{LG}) = m-1) \quad (\text{A.4})$$

by the probability that is really playing a role in this particular step of the recursion, i.e.,

$$Q_\beta^{N-k,l-1}(|\text{CLG}| < k). \quad (\text{A.5})$$

This latter probability is a quantile of the distribution of the length of the LG, and this fundamental distribution is given in (8). The required quantile of the distribution of the length of the LG is thus obtained by summing the $Q_\beta^{N-k,l-1}(\cdot)$ probabilities for $|\text{CLG}| = j$ for $j = 1, 2, \dots, (k-1)$.

Defining the Kronecker Delta symbol $\delta_{a,b}$ by

$$\delta_{a,b} = \begin{cases} 1, & \text{if } b = a \\ 0, & \text{if } b \neq a \end{cases} \quad (\text{A.6})$$

one has the initialization

$$Q_\beta^{N,l=0}(|\text{CLG}| = k, \#(\text{LG}) = m) = \delta_{k,N} \delta_{m,1} + (1 - \delta_{k,N}) \delta_{m,0}. \quad (\text{A.7})$$

Recall that

$$Q_\beta^{N,l}(X_1 = j) = \binom{N-j-1}{l-1} / \binom{N-1}{l} \quad (\text{A.8})$$

for all $1 \leq j \leq k$ [see the remarks following (7)].

At this point, we may focus our attention on the computation of the conditional probabilities

$$Q_{\beta}^{N,l;k,m}(\mathcal{G} = n) := Q_{\beta}^{N,l}(\mathcal{G} = n | |\text{CLG}| = k, \#(\text{LG}) = m) \quad (\text{A.9})$$

which, jointly with (A.3), allow for the evaluation of $Q_{\beta}^l(\mathcal{G} = n)$ using the formula for total probabilities. The conditional probabilities $Q_{\beta}^{N,l;k,m}(\mathcal{G} = n)$ are set to 0 whenever the conditioning event has a probability of 0. If the conditioning event has a positive probability, we evaluate

$$\begin{aligned} Q_{\beta}^{N,l;k,m}(\mathcal{G} = n) &= Q_{\beta}^{N,l;k,m}(X_1 = k) \\ &\times \left\{ \frac{1}{m} \delta_{n,0} + \frac{m-1}{m} Q_{\beta}^{N-k,l-1;k,m-1}(\mathcal{G} = n-k) \right\} \\ &+ \sum_{i=1}^{k-1} Q_{\beta}^{N,l;k,m}(X_1 = i) \cdot Q_{\beta}^{N-i,l-1;k,m}(\mathcal{G} = n-i). \end{aligned} \quad (\text{A.10})$$

In the RHS of (A.10), the hotspot is identified with Node 0; the initialization is given by

$$Q_{\beta}^{N,l=0;k,m}(\mathcal{G} = n) = \delta_{k,N} \delta_{m,1} \delta_{n,0} \quad (\text{A.11})$$

and we also have $Q_{\beta}^{N,l;k,m}(X_1 = k) = m/(l+1)$ (for reasons of symmetry). Furthermore, for smaller values $1 \leq i \leq k-1$, we have, using Bayes' formula

$$\begin{aligned} Q_{\beta}^{N,l;k,m}(X_1 = i) &= \frac{Q_{\beta}^{N,l}(|\text{CLG}| = k, \#(\text{LG}) = m | X_1 = i) Q_{\beta}^{N,l}(X_1 = i)}{Q_{\beta}^{N,l}(|\text{CLG}| = k, \#(\text{LG}) = m)} \\ &= \frac{Q_{\beta}^{N-i,l-1}(|\text{CLG}| = k, \#(\text{LG}) = m)}{Q_{\beta}^{N,l}(|\text{CLG}| = k, \#(\text{LG}) = m)} Q_{\beta}^{N,l}(X_1 = i) \end{aligned} \quad (\text{A.12})$$

whereby we have used that by merging the first gap

$$\begin{aligned} Q_{\beta}^{N,l}(|\text{CLG}| = k, \#(\text{LG}) = m, X_1 = i) &= Q_{\beta}^{N-i,l-1}(|\text{CLG}| = k, \#(\text{LG}) = m). \end{aligned} \quad (\text{A.13})$$

Note that the quantities appearing on the RHS of (A.12) were computed in (A.3). There are some restrictions on the range of the variables k and m : One should only consider situations where $\lceil N/(l+1) \rceil \leq k \leq (N-n)$ and $1 \leq m \leq \max\{\lfloor N/k \rfloor, (l+1)\}$ (in all other cases, the corresponding probabilities vanish).

APPENDIX B PROOF OF LEMMA 3.1

Proof: Since we are investigating the uniform, hotspot destination, and hotspot source traffic types separately, we can

rename the nodes for uniform traffic, such that the sender is node N , i.e., $S = N$. Moreover, concerning the positions and lengths of the gaps, the sender has the same effect as a receiver. Hence, we do not have to differentiate between the different types of traffic. Consider the set of active nodes $\mathcal{A} := \mathcal{F} \cup \{S\}$. Since we have renamed the nodes for uniform traffic, we now always have $N \in \mathcal{A}$.

Let K_n denote the number of active nodes between the nodes N and n (clockwise), i.e.,

$$K_n := |\mathcal{A} \cap \{1, \dots, (n-1)\}|. \quad (\text{B.1})$$

For $1 \leq l \leq N-1$ and $0 \leq k \leq (n-1) \wedge (l-1)$, we denote by $p^{l,k}$ the probability measure \mathbb{P}_x conditioned on $|\mathcal{F}| = l$ and $K_n = k$ for $x \in \{\alpha, \beta, \gamma\}$. Notice that this probability measure does not depend on the particular type of traffic x .

Assume now that the CLG starts at node n , i.e., $\mathcal{G} = n$. This implies that $\mathcal{G} \geq n$ and $n \in \mathcal{A}$. Hence, we obtain

$$\begin{aligned} p^{l,k}(\mathcal{G} = n) &= p^{l,k}(\mathcal{G} = n, \mathcal{G} \geq n, n \in \mathcal{A}) \\ &= p^{l,k}(\mathcal{G} = n | \mathcal{G} \geq n, n \in \mathcal{A}) p^{l,k}(\mathcal{G} \geq n | n \in \mathcal{A}) p^{l,k}(n \in \mathcal{A}). \end{aligned} \quad (\text{B.2})$$

We can now directly estimate the first and third factors of this expression.

Since we know that the CLG starts at a node with index n or higher, each of the remaining $(l-k)$ gaps, including the gap starting at node n , has the same chance to be the chosen largest one. Hence

$$p^{l,k}(\mathcal{G} = n | \mathcal{G} \geq n, n \in \mathcal{A}) = \frac{1}{l-k}. \quad (\text{B.3})$$

Moreover, with the conditions for $p^{l,k}$, namely $|\mathcal{F}| = l$ and $K_n = k$, there are $(l-k)$ active nodes left in $\{n, \dots, N-1\}$, and each of these $(N-n)$ nodes has the same chance of being active. Hence

$$p^{l,k}(n \in \mathcal{A}) = \frac{l-k}{N-n}. \quad (\text{B.4})$$

If we manage to show that

$$p^{l,k}(\mathcal{G} \geq n | n \in \mathcal{A}) \geq p^{l,k}(\mathcal{G} \geq n) \quad (\text{B.5})$$

then (B.2) leads to

$$p^{l,k}(\mathcal{G} = n) \geq \frac{1}{N-n} p^{l,k}(\mathcal{G} \geq n). \quad (\text{B.6})$$

Summing out the condition ($K_n = k$) yields the statement of the lemma.

It remains to prove inequality (B.5). We employ the notation

$$\mathcal{A} = \{X_1, X_2, \dots, X_l\} \quad (\text{B.7})$$

where $1 \leq X_1 < X_2 < \dots < X_l \leq N$. Therefore, the first active node with an index that is larger than or equal to n is X_{k+1} .

Since we condition on the CLG to start after n , we know that it also starts after X_{k+1} . We decompose the probability on the left-hand side of (B.5) with respect to the possible positions of X_{k+1} . We obtain

$$p^{l,k}(\mathcal{G} \geq n) = \sum_{i=n}^{N-(l-k)} p^{l,k}(\mathcal{G} \geq i | X_{k+1} = i) p^{l,k}(X_{k+1} = i) \tag{B.8}$$

$$\leq p^{l,k}(\mathcal{G} \geq n | X_{k+1} = n) \sum_{i=n}^{N-(l-k)} p^{l,k}(X_{k+1} = i) \tag{B.9}$$

$$= p^{l,k}(\mathcal{G} \geq n | X_{k+1} = n). \tag{B.10}$$

The inequality holds since the probability

$$p^{l,k}(\mathcal{G} \geq i | X_{k+1} = i) \tag{B.11}$$

is monotone decreasing in $i \in \{n, \dots, N - (l - k)\}$ since increasing i leaves less space for the $(l - k - 1)$ nodes after i and simultaneously increases the length of the last gap before i by one unit. ■

REFERENCES

[1] IEEE, *IEEE Std. 802.17: Resilient Packet Ring*, Sep. 2004. [Online]. Available: <http://ieee802.org/17>

[2] F. Davik, M. Yilmaz, S. Gjessing, and N. Uzun, "IEEE 802.17 resilient packet ring tutorial," *IEEE Commun. Mag.*, vol. 42, no. 3, pp. 112–118, Mar. 2004.

[3] S. Spadaro, J. Solé-Pareta, D. Careglio, K. Wajda, and A. Szymański, "Positioning of the RPR standard in contemporary operator environments," *IEEE Netw.*, vol. 18, no. 2, pp. 35–40, Mar./Apr. 2004.

[4] P. Yuan, V. Gambiroza, and E. Knightly, "The IEEE 802.17 media access protocol for high-speed metropolitan-area resilient packet rings," *IEEE Netw.*, vol. 18, no. 3, pp. 8–15, May/June 2004.

[5] G. Feng, C. K. Siew, and T.-S. P. Yum, "Architectural design and bandwidth demand analysis for multiparty videoconferencing on SONET/ATM rings," *IEEE J. Sel. Areas Commun.*, vol. 20, no. 8, pp. 1580–1588, Oct. 2002.

[6] R. Beverly and K. Claffy, "Wide-area IP multicast traffic characterization," *IEEE Netw.*, vol. 17, no. 1, pp. 8–15, Jan./Feb. 2003.

[7] K. Sarac and K. Almeroth, "Monitoring IP multicast in the Internet: Recent advances and ongoing challenges," *IEEE Commun. Mag.*, vol. 43, no. 10, pp. 85–91, Oct. 2005.

[8] G. N. Rouskas, "Optical layer multicast: Rationale, building blocks, and challenges," *IEEE Netw.*, vol. 17, no. 1, pp. 60–65, Jan./Feb. 2003.

[9] L. Sahasrabudhe and B. Mukherjee, "Multicast routing algorithms and protocols: A tutorial," *IEEE Netw.*, vol. 14, no. 1, pp. 90–102, Jan./Feb. 2000.

[10] M. Maier, M. Scheutzw, M. Herzog, and M. Reisslein, "Multicasting in IEEE 802.17 resilient packet ring," *J. Opt. Netw.*, vol. 5, no. 11, pp. 841–857, Nov. 2006.

[11] F. Alharbi and N. Ansari, "A novel fairness algorithm for resilient packet ring networks with low computational and hardware complexity," in *Proc. IEEE LANMAN*, Apr. 2004, pp. 11–14.

[12] F. Alharbi and N. Ansari, "SSA: Simple scheduling algorithm for resilient packet ring networks," *Proc. Inst. Elect. Eng.—Commun.*, vol. 153, no. 2, pp. 183–188, Apr. 2006.

[13] F. Davik and S. Gjessing, "The stability of the resilient packet ring aggressive fairness algorithm," in *Proc. IEEE LANMAN*, Apr. 2004, pp. 17–22.

[14] V. Gambiroza, P. Yuan, L. Balzano, Y. Liu, S. Sheafor, and E. Knightly, "Design, analysis, and implementation of DVSR: A fair high-performance protocol for packet rings," *IEEE/ACM Trans. Netw.*, vol. 12, no. 1, pp. 85–102, Feb. 2004.

[15] S. Khorsandi, A. Shokrani, and L. Lambadaris, "A new fairness model for resilient packet rings," in *Proc. IEEE ICC*, May 2005, vol. 1, pp. 288–294.

[16] Y. F. Robichaud and C. Huang, "Improved fairness algorithm to prevent tail node induced oscillations in RPR," in *Proc. IEEE ICC*, May 2005, vol. 1, pp. 402–406.

[17] Y. Robichaud, C. Huang, J. Yang, and H. Peng, "Access delay performance of resilient packet ring under bursty periodic class B traffic load," in *Proc. IEEE ICC*, Jun. 2004, vol. 2, pp. 1217–1221.

[18] A. Shokrani, S. Khorsandi, L. Lambadaris, and L. Khan, "Virtual queuing: An efficient algorithm for bandwidth management in resilient packet rings," in *Proc. IEEE ICC*, May 2005, vol. 2, pp. 982–988.

[19] A. Shikrani, I. Lambadaris, and J. Talim, "On modeling of fair rate calculation in resilient packet rings," in *Proc. IEEE Symp. Comput. Commun.*, Jun. 2005, pp. 651–657.

[20] L. Tan, H. Wang, and M. Zukerman, "Adaptive bandwidth allocation for metropolitan and wide-area networks," *IEEE Commun. Lett.*, vol. 9, no. 6, pp. 561–563, Jun. 2005.

[21] D. Wang, K. K. Ramakrishnan, and C. Kalmanek, "Congestion control in resilient packet rings," in *Proc. IEEE ICNP*, Oct. 2004, pp. 108–117.

[22] S. Zhou, M. Chen, and F. Ao, "Bandwidth utilization and fairness policy analysis of resilient packet ring," in *Proc. IEEE Int. Conf. Commun., Circuits Syst.*, May 2005, pp. 590–592.

[23] C. Huang, H. Peng, F. Yuan, and J. Hawkins, "A steady state bound for resilient packet rings," in *Proc. IEEE GLOBECOM*, Dec. 2003, vol. 7, pp. 4054–4058.

[24] C. Huang, H. Peng, and F. Yuan, "A deterministic bound for the access delay of resilient packet rings," *IEEE Commun. Lett.*, vol. 9, no. 1, pp. 87–89, Jan. 2005.

[25] D. Wang, K. Ramakrishnan, C. Kalmanek, R. Doverspike, and A. Smiljanic, "Congestion control in resilient packet rings," in *Proc. IEEE ICNP*, 2004, pp. 108–117.

[26] J. Zhu, A. Matrawy, and I. Lambadaris, "A new scheduling scheme for resilient packet ring networks with single transit buffer," in *Proc. IEEE GLOBECOM Workshops*, Nov./Dec. 2004, pp. 276–280.

[27] A. Kvalbein and S. Gjessing, "Analysis and improved performance of RPR protection," in *Proc. IEEE ICON*, Nov. 2004, vol. 1, pp. 119–124.

[28] A. Kvalbein and S. Gjessing, "Protection of RPR strict order traffic," in *Proc. IEEE Workshop Local Metropolitan Area Netw.*, Sep. 2005, pp. 1–6.

[29] X. Zhou, P. Wang, and L. Zeng, "Survivability of resilient packet rings," in *Proc. IEEE Int. Conf. Commun., Circuits Syst.*, May 2005, pp. 635–638.

[30] R. Berry and E. Modiano, "Optimal transceiver scheduling in WDM/TDM networks," *IEEE J. Sel. Areas Commun.*, vol. 23, no. 8, pp. 1479–1495, Aug. 2005.

[31] H. Liu and F. A. Tobagi, "Traffic grooming in WDM SONET UPSR rings with multiple line speeds," in *Proc. IEEE INFOCOM*, Mar. 2005, pp. 718–729.

[32] X.-Y. Li, P.-J. Wan, and L. Liu, "Select line speeds for single-hub SONET/WDM ring networks," in *Proc. IEEE Int. Conf. Commun.*, Jun. 2000, pp. 495–499.

[33] S. Subramaniam, M. Azizoglu, and A. Somani, "On the optimal placement of wavelength converters in wavelength-routed networks," in *Proc. IEEE INFOCOM*, Mar. 1998, pp. 902–909.

[34] J. Wang, W. Cho, V. R. Vemuri, and B. Mukherjee, "Improved approaches for cost-effective traffic grooming in WDM ring networks: ILP formulations and single-hop and multihop connections," *J. Lightw. Technol.*, vol. 19, no. 11, pp. 1645–1653, Nov. 2001.

[35] Y. Xu and X. Yao, "Lower bound on number of ADMs in WDM rings with nonuniform traffic demands," *Electron. Lett.*, vol. 40, no. 13, pp. 824–825, Jun. 2004.

[36] X. Zhang and C. Qiao, "An effective and comprehensive approach for traffic grooming and wavelength assignment in SONET/WDM rings," *IEEE/ACM Trans. Netw.*, vol. 8, no. 5, pp. 608–617, Oct. 2000.

[37] A. Zapata, M. Duser, J. Spencer, P. Bayvel, I. deMiguel, D. Breuer, N. Hanik, and A. Gladisch, "Next-generation 100-gigabit metro Ethernet (100 GbME) using multiwavelength optical rings," *J. Lightw. Technol.*, vol. 22, no. 11, pp. 2420–2434, Nov. 2004.

[38] M. A. Marsan, A. Bianco, E. Leonardi, M. Meo, and F. Neri, "On the capacity of MAC protocols for all-optical WDM multi-rings with tunable transmitters and fixed receivers," in *Proc. IEEE INFOCOM*, Mar. 1996, vol. 3, pp. 1206–1216.

[39] M. Scheutzw, P. Seeling, M. Maier, and M. Reisslein, "Multicast capacity of packet-switched ring WDM networks," in *Proc. IEEE INFOCOM*, Miami, FL, Mar. 2005, vol. 1, pp. 706–717.

[40] M. Veeraraghavan, H. Lee, J. Anderson, and K. Y. Eng, "A network throughput comparison of optical metro ring architectures," in *Proc. OFC*, Mar. 2002, pp. 763–765.

- [41] A. A. M. Saleh and J. M. Simmons, "Architectural principles of optical regional and metropolitan access networks," *J. Lightw. Technol.*, vol. 17, no. 12, pp. 2431–2448, Dec. 1999.
- [42] I. Rubin and H. Hua, "Synthesis and throughput behaviour of WDM meshed-ring networks under nonuniform traffic loading," *J. Lightw. Technol.*, vol. 15, no. 8, pp. 1513–1521, Aug. 1997.
- [43] M. Chaitou, G. Hebuterne, and H. Castel, "Modelling multi-channel optical slotted rings With fixed transmitter and fixed receivers," in *Proc. Adv. Ind. Conf. Telecommun./Service Assurance with Partial Intermittent Resources Conf./ E-Learning Telecommun. Workshop*, Jul. 2005, pp. 115–120.
- [44] J. He, S.-H. G. Chan, and D. H. K. Tsang, "Multicasting in WDM networks," *IEEE Commun. Surveys Tut.*, vol. 4, no. 1, 3rd Quarter 2002.
- [45] M. Herzog, M. Maier, and M. Reisslein, "Metropolitan area packet-switched WDM networks: A survey on ring systems," *IEEE Commun. Surveys Tut.*, vol. 6, no. 2, pp. 2–20, 2nd Quarter 2004.
- [46] M. Boroditsky, C. F. Lam, S. L. Woodward, N. J. Frigo, and M. D. Feuer, "Power management for enhanced system performance of passive optical rings," *Proc. Inst. Elect. Eng.—Optoelectron.*, vol. 150, no. 3, pp. 229–234, Jun. 2003.
- [47] S. Aleksic and K. Bengi, "Multicast-capable access nodes for slotted photonic ring networks," in *Proc. ECOC*, Sep. 2000, pp. 83–84.
- [48] A. Carena, V. D. Feo, J. M. Finochietto, R. Gaudino, F. Neri, C. Pigliione, and P. Poggiolini, "RingO: An experimental WDM optical packet network for metro applications," *IEEE J. Sel. Areas Commun.*, vol. 22, no. 8, pp. 1561–1571, Oct. 2004.
- [49] E. Shimada, S. Fujiwara, K. Okazaki, and I. Sasase, "A transmission system for multicast traffic with preallocation scheme in WDM ring networks," in *Proc. IEEE Pacific Rim Conf. Commun., Comput. Signal Process.*, Aug. 2003, pp. 490–493.
- [50] M. Chaitou, G. Hebuterne, and H. Castel, "Performance and multicast in WDM slotted ring networks," *Comput. Commun.*, vol. 30, no. 2, pp. 219–232, Jan. 2007.
- [51] H. Zähle, M. Scheutzow, M. Reisslein, and M. Maier, "On the multicast capacity of unidirectional and bidirectional packet-switched WDM ring networks," *IEEE J. Sel. Areas Commun.*, vol. 25, no. 4, pp. 105–119, Apr. 2007.
- [52] I. Ferrel, A. Mettler, E. Miller, and R. Libeskind-Hadas, "Virtual topologies for multicasting with multiple originators in WDM networks," *IEEE/ACM Trans. Netw.*, vol. 14, no. 1, pp. 183–190, Feb. 2006.
- [53] C. Zhou and Y. Yang, "Wide-sense nonblocking multicast in a class of regular optical WDM networks," *IEEE Trans. Commun.*, vol. 50, no. 1, pp. 126–134, Jan. 2002.
- [54] R. Ul-Mustafa and A. Kamal, "Design and provisioning of WDM networks with multicast traffic grooming," *IEEE J. Sel. Areas Commun.*, vol. 24, no. 4, pp. 37–53, Apr. 2006.
- [55] J. Wang, B. Chen, and R. Uma, "Dynamic wavelength assignment for multicast in all-optical WDM networks to maximize the network capacity," *IEEE J. Sel. Areas Commun.*, vol. 21, no. 8, pp. 1274–1284, Oct. 2003.
- [56] J. Wang, X. Qi, and B. Chen, "Wavelength assignment for multicast in all-optical WDM networks with splitting constraints," *IEEE/ACM Trans. Netw.*, vol. 14, no. 1, pp. 169–182, Feb. 2006.
- [57] X. Qin and Y. Yang, "Multicast connection capacity of WDM switching networks with limited wavelength conversion," *IEEE/ACM Trans. Netw.*, vol. 12, no. 3, pp. 526–538, Jun. 2004.
- [58] A. Bianco, J. M. Finochietto, G. Giarratana, F. Neri, and C. Pigliione, "Measurement-based reconfiguration in optical ring metro networks," *J. Lightw. Technol.*, vol. 23, no. 10, pp. 3156–3166, Oct. 2005.
- [59] H. Elbiaze and O. Cherkaoui, "Exploiting self-similar traffic analysis in network resource control: The IP over WDM networks case," in *Proc. IEEE ICAS-ICNS*, Oct. 2005, pp. 65–71.
- [60] A. Elwalid, D. Mitra, I. Saniee, and I. Widjaja, "Routing and protection in GMPLS networks: From shortest paths to optimized designs," *J. Lightw. Technol.*, vol. 21, no. 11, pp. 2828–2838, Nov. 2003.
- [61] A. Gencata and B. Mukherjee, "Virtual-topology adaptation for WDM mesh networks under dynamic traffic," *IEEE/ACM Trans. Netw.*, vol. 11, no. 2, pp. 236–247, Apr. 2003.
- [62] E. Oki, K. Shiimoto, S. Okamoto, W. Imajuku, and N. Yamanaka, "Heuristic multi-layer optimum topology design scheme based on traffic measurement for IP + photonic networks," in *Proc. OFC*, Mar. 2002, pp. 104–105.
- [63] A. Lee, D. K. Hunter, D. G. Smith, and D. Marcenac, "Heuristic for setting up a stack of WDM rings with wavelength reuse," *J. Lightw. Technol.*, vol. 18, no. 4, pp. 521–529, Apr. 2000.
- [64] A. M. Hill, M. Brierley, R. M. Percival, R. Wyatt, D. Pitcher, K. M. I. Pati, I. Hall, and J.-P. Laude, "Multiple-star wavelength-router network

and its protection strategy," *IEEE J. Sel. Areas Commun.*, vol. 16, no. 7, pp. 1134–1145, Sep. 1998.

- [65] M. Maier, M. Herzog, M. Scheutzow, and M. Reisslein, "PROTECTORATION: A fast and efficient multiple-failure recovery technique for resilient packet ring (RPR) using dark fiber," *J. Lightw. Technol.—Special Issue Optical Networks*, vol. 23, no. 10, pp. 2816–2838, Oct. 2005.



Matthias an der Heiden received the degree in mathematics and physics with a specialization in probability theory from the University of Dortmund, Dortmund, Germany. He is currently working toward the Ph.D. degree at the Department of Mathematics, Technical University of Berlin, Berlin, Germany.

Since October 2005, he has been a member of the DFG Research Center Matheon, Berlin. His research interests include metastable behavior of Markov chains, as well as mathematical aspects of network modeling.



Michel Sortais received the degree in mathematics and the Ph.D. degree with specialization in probability theory and statistical mechanics from the Swiss Federal Institute of Technology, Lausanne, Switzerland, in 2001.

Since then, he has been a Teaching and Research Assistant with the Department of Mathematics, Technical University of Berlin, Berlin, Germany. In October 2002, he joined the DFG Research Center Matheon, Berlin. His current research interests include engineering applications of probability, such as queueing theory and mobility models.



Michael Scheutzow received the Diploma in mathematics from Johann-Wolfgang-Goethe University, Frankfurt/Main, Germany, in 1979 and the Ph.D. degree in mathematics (*magna cum laude*) and the Habilitation in mathematics from the University of Kaiserslautern, Kaiserslautern, Germany, in 1983 and 1988, respectively.

From 1988 to 1990, he was a Project Leader with Tecmath GmbH, Kaiserslautern. Since 1990, he has been a Professor of stochastics with the Department of Mathematics, Technical University of Berlin, Berlin, Germany. From 1997 to 1999, he was the Associate Chair of the department. He has visited Southern Illinois University, Carbondale, IL; Rutgers University, New Brunswick, NJ; the University of Rochester, Rochester, NY; Warwick University, Coventry, U.K.; Arizona State University, Tempe; the University of California, Irvine; and the Mathematical Sciences Research Institute, University of California, Berkeley. His current research interests include stochastic differential equations, information theory, and stochastic networks.



Martin Reisslein (A'96-S'97-M'98-SM'03) received the Dipl.-Ing. (FH) degree in electrical engineering from the Fachhochschule Dieburg, Darmstadt, Germany, in 1994 and the M.S.E. degree in electrical engineering and the Ph.D. degree in systems engineering from the University of Pennsylvania, Philadelphia, in 1996 and 1998, respectively.

He is currently an Associate Professor with the Department of Electrical Engineering, Arizona State University (ASU), Tempe. During 1994–1995, he visited the University of Pennsylvania as a Fulbright scholar. From July 1998 to October 2000, he was a Scientist with the German National Research Center for Information Technology (GMD FOKUS), Berlin, Germany, and a Lecturer with the Technical University of Berlin. From October 2000 to August 2005, he was an Assistant Professor with ASU. He maintains an extensive library of video traces for network performance evaluation, including traces of MPEG-4 and H.264/AVC encoded video, at <http://trace.eas.asu.edu>. His research interests include Internet quality of service, video traffic characterization, wireless networking, optical networking, and engineering education.

Mr. Reisslein was the Editor-in-Chief of the *IEEE Communications Surveys and Tutorials* from January 2003 to February 2007.



Patrick Seeling received the Dipl.-Ing. degree in industrial engineering and management (specializing in electrical engineering) from the Technical University of Berlin (TUB), Berlin, Germany, in 2002 and the Ph.D. degree in electrical engineering from Arizona State University, Tempe, in 2005.

He is currently an Adjunct Faculty with the Department of Electrical Engineering, Arizona State University. His research interests are video communications in wired and wireless networks as well as optical networking.



Martin Herzog received the Dipl.-Ing. and Dr.-Ing. degrees from the Technical University of Berlin, Berlin, Germany, in 2002 and 2006, respectively.

During his Ph.D. studies, he received a scholarship from an interdisciplinary graduate school limited to outstanding students. He is currently a Postdoctoral Researcher with the Institut National de la Recherche Scientifique, Montréal, QC, Canada. His current research interests include architectures and protocols for access and metropolitan area optical networks.



Martin Maier (M'03) received the Dipl.-Ing. and Dr.-Ing. degrees (both with distinctions) in electrical engineering from the Technical University of Berlin, Berlin, Germany, in 1998 and 2003, respectively.

Since 2005, he has been an Associate Professor with the Institut National de la Recherche Scientifique, Montréal, QC, Canada. In summer 2003, he was a Postdoctoral Fellow with the Massachusetts Institute of Technology, Cambridge. From October 2006 to March 2007, he was a Visiting Professor with Stanford University, Stanford,

CA. He is author of the book *Metropolitan Area WDM Networks—An AWG Based Approach* (Norwell, MA: Springer, 2003). His research interests include network and node architectures; routing and switching paradigms; protection; restoration; multicasting; and the design, performance evaluation, and optimization of MAC protocols for optical wavelength-division multiplexing (WDM) networks; automatically switched optical networks; and generalized multiprotocol label switching, with particular focus on metro and access networks. His current research interests are evolutionary WDM upgrades of optical metro ring networks and access networks.

Dr. Maier served on the Technical Program Committees of the IEEE INFOCOM, IEEE GLOBECOM, IEEE ICC, and IEEE IPCCC. He is an Editorial Board Member of the *IEEE Communications Surveys and Tutorials*. He was a recipient of the two-year Deutsche Telekom doctoral scholarship from June 1999 to May 2001 and a corecipient of the Best Paper Award presented at The International Society of Optical Engineers Photonics East 2000-Terabit Optical Networking Conference.